Preprint - Accepted for publication at IEEE IROS 2019

Design of a Novel Gripper System with 3D- and Inkjet-printed Multimodal Sensors for Automated Grasping of a Forestry Robot

Lisa-Marie Faller*, Christian Stetco* and Hubert Zangl

***Abstract*— Future industrial robotic systems increasingly rely on automation of dangerous and tedious tasks. The acquisition of diverse and partially redundant information using reliable and rugged multimodal sensors helps to improve the safety an dependability of such systems. In this paper we propose proximity sensors suitable for the integration into the grasper of a forestry robot. The suggested sensor is complementary to vision based data acquisition as it can in particular provide information on objects close to the grasper that could otherwise not be obtained due to occlusion and missing direct line of sight. We present the design, fabrication and evaluation of a 3D- and inkjet-printed capacitive sensors for grasping applications in harsh industrial environment, especially forestry robotics. The sensor elements have been developed along with a complete gripper re-design. The suggested fabrication strategy allows retrofitting of various industry components and reduced maintenance and costs as well as application-specific design and optimization and are also suitable for wireless operation. The developed gripper allows the support of grasping tasks by providing proximity and contact information. A key aspect of the new system is that the spatial material distribution inside the gripper of the forestry crane can be determined and can be used for grasp quality determination. In order to support application specific adjustments such as specific location and size of the sensor electrodes, a real-time capable simulation model of the sensor system suitable to be used with environments such as VREP is also provided and demonstrated.**

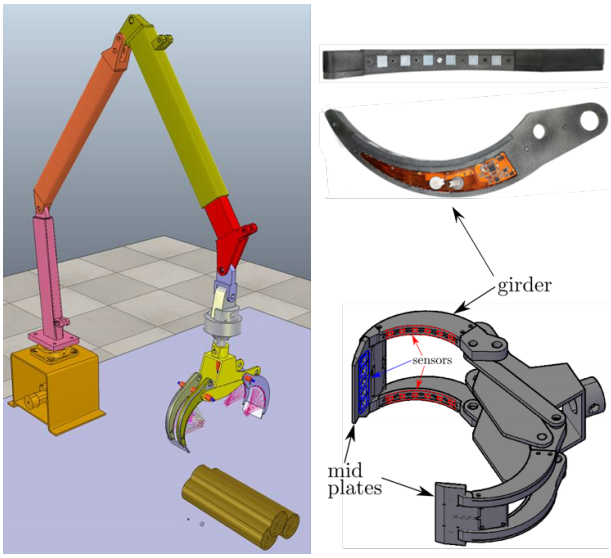

Fig. 1: Dynamic simulation model as implemented in V-REP (left), gripper design (bottom right) and photograph of the grasper prototype including the sensor elements and the wireless sensor electronics as used for the physical experiments (top right).

I. INTRODUCTION

A. Motivation

Future production as part of *industry 4.0* relies increasingly on automation [1]. This automation is, among other factors, facilitated by the employment of robots that take over tasks which are dreary, dangerous or dirty. This is especially true for high throughput industries such as agriculture and forestry [2]. Additionally, an optimization of such tasks and the related processing chain can be achieved by intelligent control and suitable sensory equipment of robotic devices, such as the hydraulic forestry crane targeted in the present work. Together with all the alleviations robotic co-workers can bring to our working environment, it is at the same time crucial to guarantee a safe co-operation with humans [3]. All of the following:

- take-over of dreary tasks
- optimize these tasks and respective processflow
- assure safe co-operation

can be achieved through additional tactile, i.e. physical, sensors - as vision alone is only of limited capability here [4]. Especially in mobile applications, without information about the environmental conditions, physical sensors show tremendous advantages as discussed and demonstrated e.g. in [5], [6]. Tactile sensors have been used proposed for robot grippers, e.g. in [7]. In this work, we employ tactile sensing for the automation of a hydraulic forestry crane (see Fig. 2), which represents a harsh environment with respect to the sensors. The aim it to support the grasping and grasp planning processes as the sensors can provide information e.g. about poor grasps. As capacitive proximity sensors do not require any moving parts and can thus withstand strong forces and mechanical impacts, are comparatively insensitive to staining and can be designed to be tolerant with respect to mechanical wear, they are promising for such applications. The principle can be beneficially applied at various stages of interaction (e.g., pre-touch, contact, manipulation and grasping, gesture control etc.).

B. Related Work

Often, existing robotic devices are retrofit with tactile sensors, e.g. in order to fabricate highly sensitive fingers such as shown in [8], or using electronic skin [9]. Tactile sensors are of special importance also in the medical context

*Authors contributed equally to this work.

The authors are with the Institute of Smart System Technologies, Sensors and Actuators Department, Alpen-Adria-Universität Klagenfurt, 9020 Klagenfurt, Austria lisa-marie.faller@aau.at

for surgical robotics [10]. Most of the related work has an emphasis on giving robots a human sense of touch [11] in order to provide them with learning and manipulation capabilities [12]–[14] as well as improve grasping [15]–[17]. Duchaine gave reasons why is believed that tactile intelligence is the future of robotic grasping in [4]. This is the more true for industrial robots, such as the one targeted in this work.

Capacitive sensing is widely used for tactile sensing, e.g. as tactile sensor based on multimodal (static and dynamic) measurements in [18], or for measurement of force in 3-axis as shown in [19].

A capacitive sensing principle is especially also useful to enable safe collaboration: In [20], a conformable robotic skin for collision avoidance is presented and in [21] a capacitively based pre-touch sensing system is shown. In [22] the authors present a grasper equipped with capacitive sensors for contour following. The multimodality that is provided by capacitive sensors is of importance also in our work and we evaluate both, proximity and touch behaviour.

Sensors based on novel materials are also topic of recent research. Rocha et al. [23] show a soft-matter sensor which combines pre-touch and pressure sensing. In [24] the authors demonstrate gecko-inspired capacitive sensors for the development of a novel robot gripper and in [25], an industrial gripper is equipped with additional friction components. In [18], the authors show a capacitive tactile sensor based on a structured dielectric.

Recently, also 3D- and inkjet-printing have been used in this context: The functionality of inkjet-printed sensors for vicinity detection and robot control has been shown in [26], [27]. In [28] the authors employ a 3D-printed gripper to show precise in-hand manipulation. Also in [29] a 3D-printed tactile fingertip sensor for manipulation is shown. Many approaches based on novel materials often present conformable systems, and target soft robotic devices. With respect to harsh environments, in [30] tactile sensors which can withstand high temperatures have been shown. However our work focuses on temperature resistant and at the same time also mechanically highly durable materials in order to provide rugged sensors giving reliable information. To this end, the combination of 3D-printed ceramics and inkjet-printed conductive layers for highly sensitivity pressure sensors has been shown [31].

The importance of developments for forestry robotics was pointed out previously [32]. A teleoperation system and benefits of such frameworks are shown in [33]. Work on the automation of log manipulation for forestry robots has been presented in [34] and also 3D log recognition and pose estimation [35], both based solely on vision. Here, the system we propose can ideally complement under changing environmental conditions and obstrued line of sight.

C. Contribution

We present a novel gripper design, based on dual-mode, i.e. touch and proximity, capacitive sensors, for autonomous industrial systems. These sensors are employed to support grasping, and are especially suited for harsh environments. We focus on a forestry robotics application in which the gripper encounters harsh conditions such as high temperature ranges, changing seasons, rain or dirt. Our system benefits from the capacitive principle which provides robust grasping information under these conditions and thus can perfectly complement optical or vision based systems. The sensor information can be used to improve the log processing speed and can significantly raise the throughput and reduce costs.

Fig. 2: Photograph of a corresponding hydraulic forestry crane at a sawmill delivery.

The sensory hardware is fabricated using 3D- and inkjet-printing. Due to the employed fabrication technologies, the sensors are suitable for retrofitting and efficient low-volume production as well as individual design optimization and adaptability. The suggested capacitive sensors can achieve high sensitivity [36] and benefit from fast, inexpensive and uncomplicated manufacturing. To sustain harsh conditions, a 3D-printed ceramic substrate is used onto which conductive layers are fabricated by inkjet-printed silver. Experimental results using a wireless capacitive sensor readout [37], [38] is also provided.

We also present a complete dynamic simulation setup of the forestry robot, gripper and sensors together with online finite element method (FEM) computations of capacitance and relative electrical permittivity. The whole setup is integrated with ROS to make the sensor data available for further applications such as grasp planning and control. Results for the computation of the material distribution are shown together with an experimental evaluation of the sensory setup.

The remainder of this paper is structured as follows: Section II gives an overview of the crane system used in this work. Next, in Section III we give a detailed description of

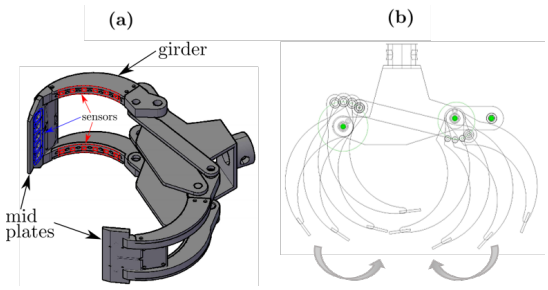

Fig. 3: (a) Gripper design with a front view of the outer (broader) side. (b) Schematic illustration of the gripper movement.

the capacitive sensor system. Section IV describes the used simulation framework for sensor and system simulation and virtualization. In Section V, we present experimental results, and finally, in Section VI the conclusion is given.

II. CRANE SYSTEM DESCRIPTION

The target forestry crane (see Fig. 2) can be used as truck-mounted mobile system, but also stationary at the delivery of saw mills. Commonly, it is steered using a complex control unit which is run by a human operator.

The crane system is mounted on a rotational base and actuated by three subsequent hydraulic piston cylinders acting as prismatic joints. Finally, the gripper is connected to the system by a rotational joint and another two unconstrained joints in which axes the gripper can move freely (similar to a yaw motion). The actuation of the gripper is also hydraulic, resulting in a force-locked connection with the grasped logs. Since the whole gripper is actuated by only one cylinder, it additionally is an underactuated mechanism.

A. Gripper Design

The design is based on two gripper parts of different dimension, as shown in Fig. 3 (a). These parts can close in a way that the narrower gripper part moves inside the clearance of the broader part (see Fig. 3 (b)). This way, a force-locked connection is possible independent on the number or size of logs inside the gripper. In order to fit the sensors and read-out electronics while maintaining this freedom in movement, the two distinct gripper parts have to be re-designed individually.

Both gripper sides are equipped with six sensors at each of the two lateral, longitudinal girders. Additionally, the broader gripper part has five sensors in the mid connection plate between the girders; the narrower gripper part holds four such sensors. The sensor read-out and communication electronics for the respective mid plates are placed in a milled recess at the back and towards the clearances on both parts of the gripper. The electronics which process the sensor signals from the sensors in the girders are placed inside a recess at the respective girder sides. The sizing of the capacitive sensors is a trade-off between achievable distance and object size resolution. The sensors are designed to cope with the smallest log size as determined by the application.

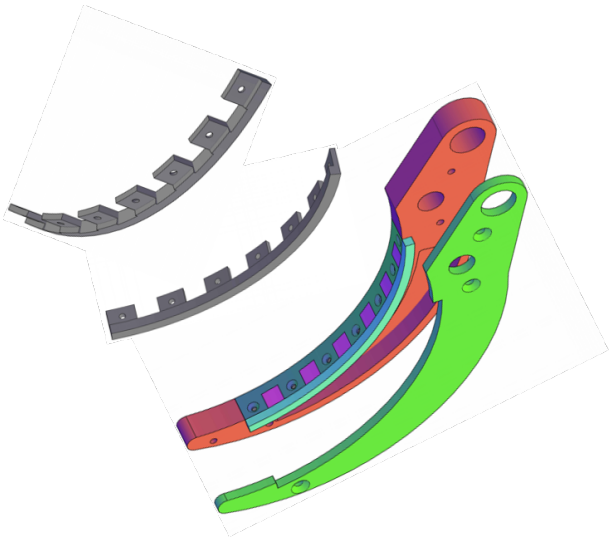

Fig. 4: Design of the girders.

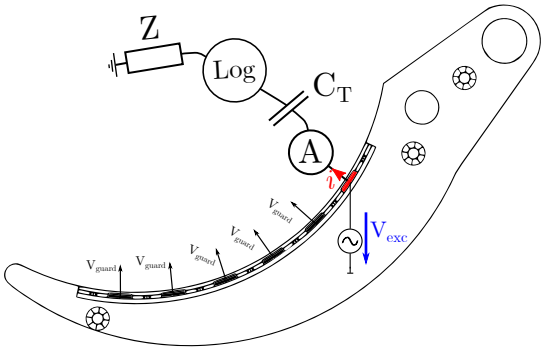

Fig. 5: Single-ended capacitive measurement principle.

B. Girders Design

Each of the four girders holds six capacitive sensors which are distributed equally spaced along the curvature of the part. The girders (Fig. 4) themselves are constructed from four base parts, the main body (Fig. 4: orange part), two interlocked inlays (Fig. 4: separately as grey parts and assembled as turquois parts) in orange which hold the sensors (Fig. 4: purple openings) and a cover (Fig. 4: green part). The inlays and cover can be removed in order to access the electronics and sensors and to keep them exchangeable in case of malfunction or damage. The clearances in the inlays are conic in order to fix the sensors accordingly inside. Behind the clearance is a through-hole which allows to electrically connect the sensing and guard layers of the capacitive sensors to the respective electronics.

III. CAPACITIVE SENSOR SYSTEM

A. Sensing Principle

Capacitive sensors rely on the basic physical principle of Maxwell's Equations. Due to changes in the electric field in the near vicinity of such sensors, a change of capacitance can be detected. A simplified mathematical description of which

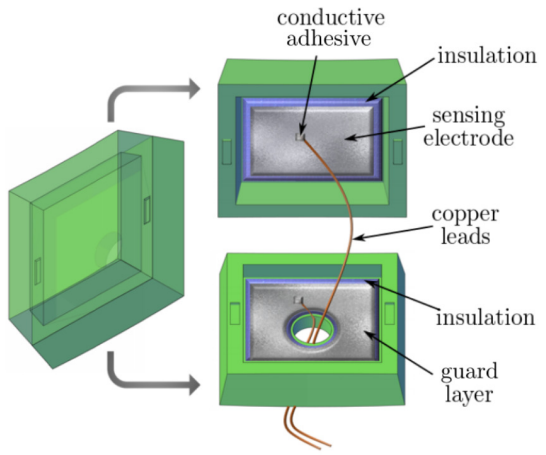

Fig. 6: Structure of the sensors as composed of the sensor top and sensor base parts. Both conductive layers and the conductive adhesive are covered by insulator again to avoid electrical shortage, this final layer is not shown in the illustration.

can be given by

$$\Delta C = \frac{\varepsilon_0 \varepsilon_r A_r}{\Delta d} \tag{1}$$

where ΔC is the change in capacitance in farads, A_r the active plate area in square meters, ϵ_0 the dielectric constant of vacuum, ϵ_r the relative dielectric constant of the material between the plates and Δd the change of the plate spacing in meters.

This can then be further processed for applications such as proximity sensing for collision avoidance [39], as near-field sensors in tomographic applications or as touch sensor elements. Such sensors commonly consist of a multitude of electrodes in various configurations, depending on the scenario, which are driven by an excitation signal either in differential-mode or single-ended mode (compare e.g., [40]). In single-ended mode, the displacement current at the transmitter, i.e. the excited electrode, is measured, while the remaining electrodes are kept at a constant potential. Single-ended measurements are advantageous in proximity sensing applications to the open environment and consequently are implemented in the target gripper. To ensure correct sensor operation, shielding or guarding must be provided at the sensor electrodes, evaluation circuitry and sensor leads. The guarding provides robustness against parasitic effects. A schematic setup of the capacitive sensor principle is shown in Fig. 5. Here, a single electrode is excited and the displacement current (i) at the transmitting electrode is measured. If an object approaches the electrode, the capacitance change can be measured via the change of the respective displacement current. Additionally, also a permittivity distribution can be reconstructed using this principle. The relative electrical permittivity ϵ_r is a material property and, roughly speaking, gives the resistance of a material against its penetration with electric field lines.

B. Sensor Design and Fabrication

The sensors consist of two parts superposed to each other. On the inner part, which is the sensor base, the guard layer is applied, it also has a through-hole at the center to enable electrical connection. The outer part, which is the sensor top, holds the sensing electrode. The sensing electrodes and guard layer are inkjet-printed onto 3D-printed substrates in a multilayer fashion. First, an insulating layer is inkjet-printed onto the substrates in order to provide a homogenous surface for the subsequent metal layers. The sensing electrodes and guard layer are then inkjet-printed onto the base insulator of the sensor base and top. The electrical connection of both layers is then achieved by fixing wires with thermally curable conductive adhesive. The whole sensor part has a conical outline so that it is properly fixed inside the inlay.

C. Read-Out Hardware

For signal processing and data transmission a hardware layout was designed which is fully integrated into each girder as well as the mid plates (compare Figure 1). To meet the stringent space criteria for integration, a flexible printed circuit board (PCB) was designed. The flexible design meets the geometrical constraints on the geometrical outlines of the recesses for the PCBs in the girders and mid plates. To enable an autarkic operation of the sensors, the PCB is powered with coin batteries. The sensor data is transmitted wireless to a base station. The hardware operates the capacitive sensors in single-ended mode and excites one electrode after the other using a ramp signal. While the powered electrode is used as transmitter, the remaining ones are put to guard potential. This is achieved by time-multiplexing implemented using a switch matrix. The displacement current is measured using an I/U converter at each electrode. The signals are further amplified and converted to digital signals using an ADC converter, here a capacitance-to-digital converter (CDC) from Analog Devices [41] in single-ended operation mode is used. The frequency of the excitation signal is $f_{exc} = 32\,\mathrm{kHz}$. However, using this hardware static as well as dynamic measurements are possible.

IV. Simulation Setup

A dynamic simulation of the crane system and gripper is set up in V-REP. To generate and examine different grasp sets, a gamepad/joystick control is interfaced with the open-source 3D simulation engine V-REP [42]. Additionally, a communication between V-REP and a finite element method (FEM) simulation in Matlab is established through ROS. V-REP provides different models of proximity sensors, which in essence provide the distance to the objects. In order to mimic the behaviour of capacitive sensors, an array of point size proximity sensors in VREP is arranged to sample the geometry of the object, which is then used as the input for a fast FEM simulation which provides the corresponding capacitive sensor signals. Vortex Studio[1] is used as the physics engine. The sensor distance data acquired

[1]https://www.cm-labs.com/vortex-studio/

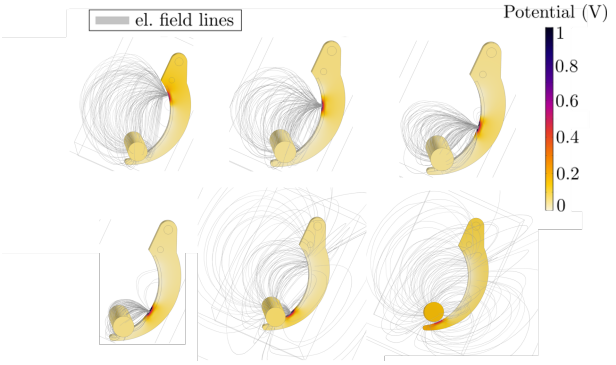

Fig. 7: Illustration of the electric field lines when each of the six sensing electrodes is used as transmitter while the others are at guard potential.

in VREP is transferred to Matlab, where we use our fast FEM imnplementation to calculate the respective capacitance values and reconstruct the permittivity distribution. These processes can run concurrently. Then, the capacitance values can be transferred back to ROS for furhter use in crane control and grasp planning.

A. Capacitance Computation and Permittivity Map

For detailed analysis and as a reference a commercial FEM solver (Comsol[2]) is used to evaluate the system behaviour and for the determination of precise capacitance values. A plot of the evolution of electric field lines around the log when each sensor is powered is given in Fig. 7.

However, a detailed 3D model employing remeshing for geometry changes is not suitable for real time simulations. Consequently, we make use of techniques to accelerate the FEM computation as they are used in Electrical Capacitance Tomography [43], [44]. Basically, in FEM the partial differential equation $\operatorname{div} \varepsilon \operatorname{grad} u = 0$ for electrostatic gets converted into a linear equation system $\mathbf{KU} = \mathbf{rhs}$, where $\mathbf{U}$ are the solutions for the electric potential u at the mesh nodes, $\mathbf{K}$ is the so-called stiffness matrix, which depends on the geometry and the material values ε and $\mathbf{rhs}$ essentially contains the boundary conditions. In order to speed up the simulation, we keep the same mesh for all simulations and include the objects by assigning corresponding material values to the mesh elements. With this, all geometry dependent sub matrices can be pre-computed allowing for a fast assembly of the stiffness matrix. In order to assign the material values each capacitive sensor is approximated by a number of (in our simulations we used three) ray-type proximity sensors within VREP with aperture angles α as shown in Fig. 8 (a). Based on this, the log outline is computed using linear regression. In the presented experiments, a quadratic function is used, requiring a minimum of three distance values (support points) corresponding to the three ray-type proximity sensors. The boundary of the log is then approximated as

$$y(x) = a_0 + a_1 x + a_2 x^2 \tag{2}$$

[2]https://www.comsol.com/

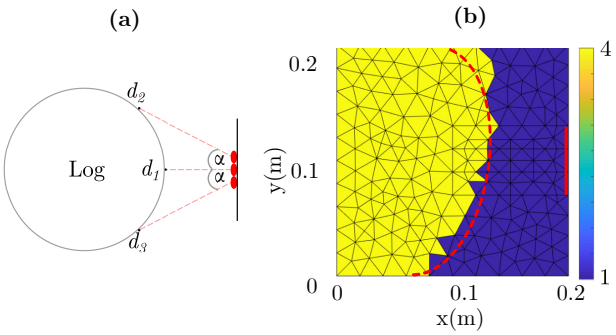

Fig. 8: (a) 2D FEM model for calculating the capacitance values of the simulated distance data. The red dots correspond to the simulated ray-based proximity sensors in V-REP. The angle α is the half the aperture angle which is set in the simulation environment. The distance values d_1, d_2 and d_3 are the obtained distance values, respectively. (b) 2D FEM reconstruction using the quadratic interpolation model. The red line on the right is the sensing electrode. The blue regions correspond to the permittivity values of air, i.e. $\varepsilon_{r,air} = 1\,\mathrm{F/m}$ whereas yellow regions correspond to a typical permittivity value of wood, i.e. $\varepsilon_{r,wood} \approx 2-4\,\mathrm{F/m}$. The dashed red line shows the true position of the log during grasping whereas the yellow regions shows the interpolated permittivity values from the simulated online distance data.

with unknown coefficients $\mathbf{a} = [a_0\ a_1\ a_2]^T$. The coordinate values are simply obtained from the aperture angle, i.e. $\mathbf{x} = \mathbf{d}\cos(\alpha)$ and $\mathbf{y} = \mathbf{d}\sin(\alpha)$, where $\mathbf{d} = [d_1\ d_2\ d_3]$, respectively. To compute the unknown coefficient vector, we employ a least-squares estimator (e.g. [45]). Accordingly, the unknown coefficient vector is obtained as

$$\mathbf{a} = (\mathbf{H}^T\mathbf{H})^{-1}\mathbf{H}^T\mathbf{y} \tag{3}$$

where $\mathbf{H} = [\mathbf{1}\mathbf{X}\mathbf{X}^2]$, and $\mathbf{X}$ represents the vector of x-coordinates of the support points. Mesh elements that are further away from the sensor than the corresponding surface approximation $y(x)$ are considered to belong to the object and we assign the corresponding material permittivity value (wood). Mesh elements which are closer, are set to the permittivity of air. An example resulting permittivity map is shown in Fig. 8 (b).

V. EXPERIMENTAL SETUP AND RESULTS

A. Grasping Experiments

To perform the grasping experiments as realistic as possible, the gripper girder was mounted on a moveable stage for accurate positioning of the logs and the gripper. Three different logs where used with diameters $d_1 = 30\,\mathrm{mm}$, $d_2 = 90\,\mathrm{mm}$ and $d_3 = 145\,\mathrm{mm}$ and equal length of $l = 1000\,\mathrm{mm}$. The experimental setup is shown in Fig. 9.

Fig. 11 shows the obtained capacitance values for grasping the small log. To further analyze the behavior, we distinguish between four different phases during grasping. In the first phase, the gripper approximates and picks up the log. Here, the first sensor detects the log and sensor two is in proximity

Fig. 9: Experimental setup for evaluation of the capacitive sensors.

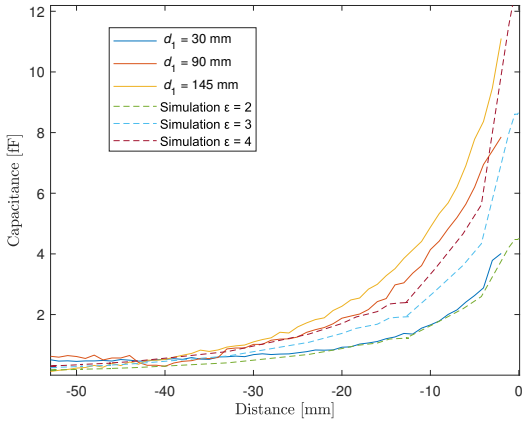

Fig. 10: Capacitance values for different logs averaged over 10 measurements for each log and real-time simulations results. The characteristic varies with size and shape of the object, the material properties and the actual aligment with respect to the sensor. The shown results apply to the scaled lab model.

mode. By further closing the gripper girders, the log slides to the inside which is obtained as phase two. Here, sensors two to five detect the log and give proximity data. After the log is grasped, the gripper reaches steady-state whereas the log tends to oscillate around sensors five and four. Depending on the closing speed, peaks in the measurements can result from the oscillating motion of the log. After the log was successfully grasped, the gripper opens which yields phase four. It is worth to mention that the closing and opening speeds of the gripper influences the capacitance values. Therefore, it is crucial to operate at moderate speeds to ensure correct sensor read-outs. Such a behavior can be seen in Fig. 11 around time $t = 11\,\mathrm{s}$ where the second sensor has only a peak value which results from a faster release of the log.

B. Sensor Sensitivity

To obtain the sensor sensitivity $s(d)$, several measurements were taken for different log positions. Hence, by adjusting the log coordinates in the (x,y) plane step-by-step, the sensitivity can be evaluated accordingly. In general, the sensitivity of a sensor is defined as the differential change of the sensor output with respect to a differential change of an input quantity. Here, we evaluate the sensitivity of the capacitance with respect to the distance of the log, i.e. $s(d) = \frac{\partial C}{\partial d}$. We analyzed one sensor element by adjusting the position of the log using incremental steps of $d_{inc} = 1\,\mathrm{mm}$ and starting at an initial position of $d_{init} = 60\,\mathrm{mm}$. The proximity range was obtained with $r_p = 50\,\mathrm{mm}$ for the big log, $r_p = 40\,\mathrm{mm}$ for the medium log and $r_p = 35\,\mathrm{mm}$ for the small log, respectively. Fig. 12 shows the obtained measurements, fitted theoretical curves and sensitivities, respectively. For fitting the measurement data C_m, a least squares algorithm was used to obtain the theoretical curve with data C_f. It is worth noting that the higher sensitivities have been obtained for larger objects in the vicinity of the sensor.

C. Proximity Behavior

To analyze the proximity behavior of the sensor elements, we used the same experimental setup as shown in Fig. 9. We evaluated the performance for one sensor module using three different logs. Hence, 10 measurements for every log have been made and the corresponding averaged capacitance values are shown in Fig. 10. The proximity range increases with increasing log diameter which is caused due to the larger object in the vicinity of the sensor. Hence, larger logs can be easier detected by the sensor system.

VI. CONCLUSION

In this paper, we present the design of an industrial gripper system with integrated capacitive multimodal 3D- and inkjet-printed sensors for automated grasping of a forestry robot. The functionality of the sensors was experimentally evaluated and their sensitivity as well as proximity and grasping behaviour were characterized. Additionally, a dynamic simulation model of the hydraulic crane for grasp set creation and grasping evaluations was presented. The simulation includes a realistic real time capable simulation model for the capacitive sensors, which allows e.g. to find application specific appropriate sensor locations and dimensions without the need of physical realization. Together with the 3D- and inkjet-printing manufacturing approach this allows for fast retrofitting but also fast design of new grippers with capacitive proximity sensors.

APPENDIX

The attached video shows the grasping of logs in V-REP and the corresponding online, FEM computed, capacitance values in Matlab.

ACKNOWLEDGMENT

The research leading to these results has received funding from the Austrian Ministry for Transport, Innovation and Technology (BMVIT) within the ICT of the Future Programme (4th call) of the Austrian Research Promotion Agency (FFG) under grant agreement n. 864807 (AutoLOG).

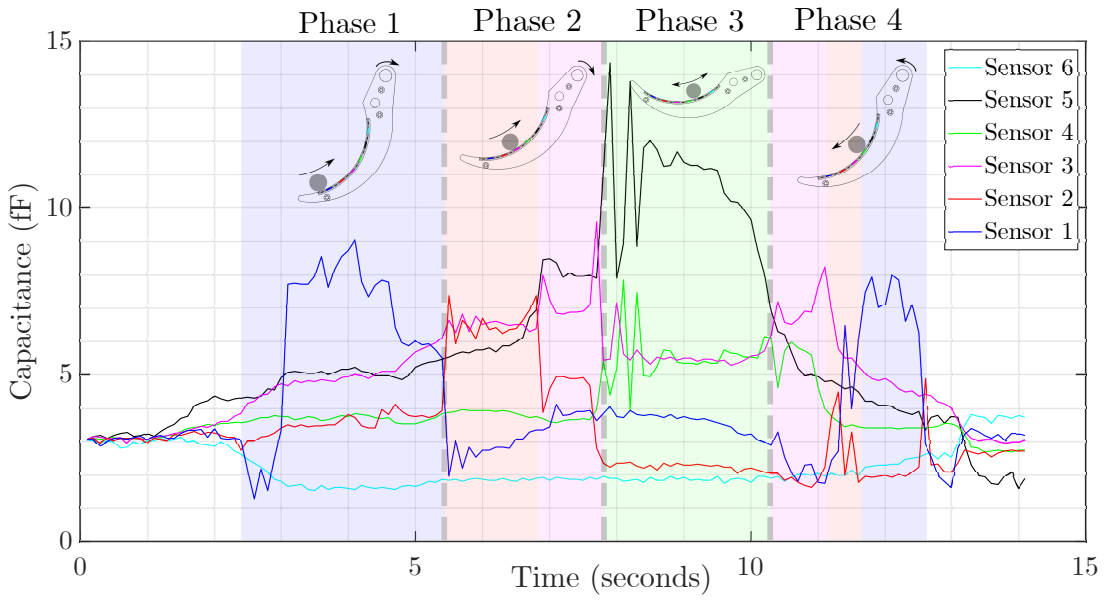

Fig. 11: Evaluation of capacitance measurements during grasping.

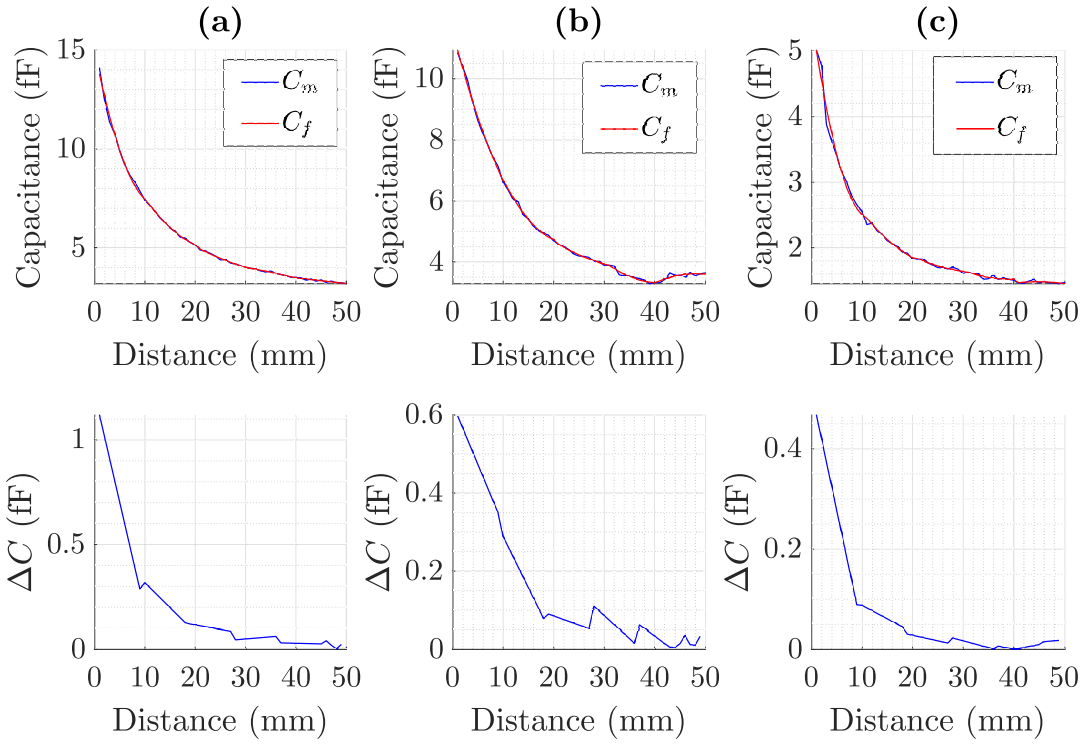

Fig. 12: Measured capacitance value (top) and the derived sensitivity values for (a) big log with diameter d_3, (b) mid log with diameter d_2 and (c) the small log with diameter d_1. Measured capacitance values are depicted in blue whereas the fitted theoretical curve is shown in red.

The authors would like to thank Aditya Kapilavai for his work on the V-REP model and valuable suggestion on the paper, and Jevgeni Ignasov, SDU Robotics, Denmark for his suggestions to V-REP simulations.

REFERENCES

[1] Y. Lu, "Industry 4.0: A survey on technologies, applications and open research issues," *J. of Industrial Information Integration*, no. 6, pp. 1–10, 2017.

[2] A. Halme and M. Vainio, *Forestry robotics - why, what and when*, 2005, pp. 149–162.

[3] M. Geiger and C. Waldschmidt, "160-GHz Radar Proximity Sensor With Distributed and Flexible Antennas for Collaborative Robots," *IEEE Access*, vol. 7, pp. 14 977 – 14 984, 2019.

[4] V. Duchaine, "Why tactile intelligence is the future of robotic grasping," *IEEE Spectrum*, 2016. [Online]. Available: https://spectrum.ieee.org/automaton/robotics/robotics-hardware/why-tactile-intelligence-is-the-future-of-robotic-grasping

[5] M. Kaboli and G. Cheng, "Robust Tactile Descriptors for Discriminating Objects From Textural Properties via Artificial Robotic Skin," *IEEE Trans. on Robotivs*, vol. 34, no. 4, 2018.

[6] G. Robles-De-La-Torre, "The Importance of the Sense of Touch in Virtual and Real Environments," *IEEE Multimedia*, vol. 13, no. 3, pp. 24–30, 2006.

[7] A. Schmitz, M. Maggiali, L. Natale, B. Bonino, and G. Metta, "A tactile sensor for the fingertips of the humanoid robot icub," in *Intelligent Robots and Systems (IROS), 2010 IEEE/RSJ International Conference on*, Oct 2010, pp. 2212–2217.

[8] T. P. Tomo, A. Schmitz, W. K. Wong, H. Kristanto, S. Somlor, J. Hwang, L. Jamone, and S. Sugano, "Covering a Robot Fingertip With uSkin: A Soft Electronic Skin with Distributed 3-Axis Force Sensitive Elements for Robot Hands," *IEEE Robotics and Automation Letters*, vol. 3, no. 1, pp. 124–131, 2018.

[9] A. Schmitz, P. Maiolino, M. Maggiali, L. Natale, G. Cannata, and G. Metta, "Methods and technologies for the implementation of large-scale robot tactile sensors," *Robotics, IEEE Transactions on*, vol. 27, no. 3, pp. 389–400, June 2011.

[10] P. S. Girão, P. M. P. Ramos, O. Postolache, and J. M. D. Pereira, "Tactile sensors for robotic applications," *Elsevier Measurement*, vol. 46, pp. 1257–1271, 2013.

[11] R. Dahiya, G. Metta, M. Valle, and G. Sandini, "Tactile sensing - from humans to humanoids," *Robotics, IEEE Transactions on*, vol. 26, no. 1, pp. 1–20, Feb 2010. [Online]. Available: http://ieeexplore.ieee.org/stamp/stamp.jsp?tp=&arnumber=5339133

[12] W. Fukui, F. Kobayashi, F. Kojima, H. Nakamoto, N. Imamura, T. Maeda, and H. Shirasawa, "High-speed tactile sensing for array-type tactile sensor and object manipulation based on tactile sensing," *Journal of Robotics*, 2011.

[13] A. Maldonado, H. Alvarez, and M. Beetz, "Improving robot manipulation through fingertip perception," in *Intelligent Robots and Systems (IROS), 2012 IEEE/RSJ International Conference on*, Oct 2012, pp. 2947–2954.

[14] L.-T. Jiang and J. R. Smith, "Pretouch sensing for manipulation," *Robotics: Science and Systems (RSS) Workshop: Alternative Sensing Techniques for Robotic Perception*, 2012.

[15] J. Romano, K. Hsiao, G. Niemeyer, S. Chitta, and K. Kuchenbecker, "Human-inspired grasp control with tactile sensing," *IEEE Trans. on Robotics*, vol. 27, no. 6, 2011.

[16] L. T. Jiang and J. R. Smith, "Seashell effect pretouch sensing for robotic grasping," in *IEEE Int. Conf. on Robotics and Automation*, 2012.

[17] H. Dang and P. Allen, "Stable grasping under pose uncertainty using tactile feedback," *Autonomous Robots*, vol. 36, no. 4, 2014.

[18] T.-H.-L. Le, A. Maslyczyk, J.-P. Roberge, and V. Duchaine, "A highly sensitive multimodal capacitive tactile sensor," in *IEEE Int. Conf. on Robotics and Automation (ICRA) 2017*, 2017.

[19] G. Liang, Y. Wang, D. Mei, K. Xi, and Z. Chen, "Flexible capacitive tactile sensor array with truncated pyramids as dielectric layer for three-axis force measurement," *J. of Microelectromech. Sys.*, vol. 24, pp. 1510–1519, 2015.

[20] D. Hughes, J. Lammie, and N. Correll, "A Robotic Skin for Collision Avoidance and Affective Touch Recognition," *IEEE Robotics and Automation Letters*, vol. 3, no. 3, pp. 1386–1393, 2018.

[21] B. Mayton, L. LeGrand, and J. Smith, "An electric field pretouch system for grasping and co-manipulation," in *Robotics and Automation (ICRA), 2010 IEEE International Conference on*, May 2010, pp. 831–838. [Online]. Available: http://ieeexplore.ieee.org/stamp/stamp.jsp?tp=\&arnumber=5509658

[22] S. E. Navarro, S. Koch, and B. Hein, "3d contour following for a cylindrical end-effector using capacitive proximity sensors," in *IEEE/RSJ Internat. Conf. on Intell. Robots and Systems (IROS) 2016*, 2016.

[23] R. Rocha, P. Lopes, A. T. de Almeida, M. Tavakoli, and C. Majidi, "Soft-matter sensor for proximity, tactile and pressure detection," in *IEEE/RSK Int. Conf. on Intell. Robots and Systems (IROS) 2017*, 2017.

[24] J. Hashizume, T. M. Huh, S. A. Suresh, and M. R. Cutkosky, "Capacitive Sensing for a Gripper With Gecko-Inspired Adhesive Film," *IEEE Robotics and Automation Letters*, vol. 4, no. 2, pp. 677–683, 2019.

[25] J.-P. Roberge, W. Ruotolo, V. Duchaine, and M. Cutkosky, "Improving Industrial Grippers With Adhesion-Controlled Friction," *IEEE Robotics and Automation Letters*, vol. 3, no. 2, pp. 1041–1048, 2018.

[26] S. Mühlbacher-Karrer, L.-M. Faller, H. Zangl, T. Schlegl, and M. Moser, "Short range capacitive proximity sensing," in *2nd Workshop on Alternative Sensing for Robot Perception Beyond Laser and Vision*, Hamburg, Germany, October 2015.

[27] S. Mühlbacher-Karrer, M. Brandstötter, D. Schett, and H. Zangl, "Contactless control of a kinematically redundant serial manipulator using tomographic sensors," *IEEE Robotics and Automation Letters*, vol. 2, pp. 562–569, 2017.

[28] B. Ward-Cherrier, N. Rojas, and N. F. Lepora, "Model-Free Precise in-Hand Manipulation with a 3D-Printed Tactile Gripper," *IEEE Robotics and Automation Letters*, vol. 2, no. 4, pp. 2056–2063, 2017.

[29] Z. Xu, S. Kolev, and E. Todorov, "Design, Optimization, Calibration, and a Case Study of a 3D-Printed, Low-cost Fingertip Sensor for Robotic Manipulation," in *IEEE Int. Conf. on Robotics and Automation (ICRA)*, 2014.

[30] A. Alfadhel, M. A. Khan, S. Cardos, D. Leitao, and J. Kosel, "A Magnetoresistive Tactile Sensor for Harsh Environment Applications," *Sensors*, vol. 16, no. 5, 2016.

[31] L.-M. Faller, W. Granig, M. Krivec, A. Abram, and H. Zangl, "Rapid prototyping of force/pressure sensors using 3d- and inkjet-printing," *IOP J. Micromech. Mircoeng.*, vol. 28, no. 10, 2018.

[32] M. Bergerman, B. J., R. J., and van Henten E, *Robotics in Agriculture and Forestry*, 2016, pp. 1463–1492.

[33] S. Westerberg, I. R. Manchester, U. Mettin, P. La Hera, and A. Shiriaev, "Virtual Environment Teleoperation of a Hydraulic Forestry Crane," in *Proc. of the 2008 IEEE Int. Conf. on Robotics and Automation*, 2008.

[34] L. Shao, X. Chen, B. Milne, and P. Guo, "A Novel Tree Trunk Recognition Approach for Forestry Harvesting Robot," in *Proc. of the 2014 9th IEEE Conference on Industrial Electronics and Applications*, 2014.

[35] Y. Park, A. Shiriaev, S. Westerberg, and S. Lee, "3D Log Recognition and Pose Estimation for Robotic Forestry Machine," in *Proc. of the 2011 Int. Conf. on Robotics and Automation*, 2011.

[36] L.-M. Faller, T. Mitterer, S. Weiss, and H. Zangl, "3d- and inkjet-printed force sensors for tactile sensing," in *RoboTac: Workshop on Tactile Sensing and Perception, IEEE Int. Conf. on Intelligent Robots and Systems (IROS)*, 2018.

[37] T. Schlegl, M. Moser, and H. Zangl, "Wireless and flexible ice detection on aircraft," in *International Conference on Icing of Aircraft, Engines, and Structures*. Prague, Czech Republic: SAE, June 2015.

[38] S. Mhlbacher-Karrer, A. H. Mosa, L. Faller, M. Ali, R. Hamid, H. Zangl, and K. Kyamakya, "A driver state detection systemcombining a capacitive hand detection sensor with physiological sensors," *IEEE Transactions on Instrumentation and Measurement*, vol. 66, no. 4, pp. 624–636, April 2017.

[39] T. Schlegl, T. Krger, A. Gaschler, O. Khatib, and H. Zangl, "Virtual whiskers highly responsive robot collision avoidance," in *2013 IEEE/RSJ International Conference on Intelligent Robots and Systems*, Nov 2013, pp. 5373–5379.

[40] L. Baxter, *Capacitive Sensors, Design and Applications*. IEEE Press, 1997.

[41] *Programmable Controller for Capacitance Touch Sensors AD7142, Datasheet*, Analog Devices.

[42] E. Rohmer, S. P. N. Singh, and M. Freese, "V-REP: a Versatile and Scalable Robot Simulation Framework," in *Proc. of The International Conference on Intelligent Robots and Systems (IROS)*, 2013.

[43] M. Neumayer, H. Zangl, D. Watzenig, and A. Fuchs, "Current reconstruction algorithms in electrical capacitance tomography," in *New Developments and Applications in Sensing Technology*, ser. Lecture Notes in Electrical Engineering. Springer Berlin Heidelberg, 2011, vol. 83, pp. 65–106.

[44] S. Mühlbacher-Karrer, J. Leitzke, L.-M. Faller, and H. Zangl, "Non-iterative object detection methods in electrical tomography for robotic applications," *COMPEL - The international journal for computation and mathematics in electrical and electronic engineering*, vol. 36, pp. 1411–1420, 2017.

[45] S. M. Kay, *Fundamentals of Statistical Signal Processing, Estimation Theory*. Prentice-Hall, Inc., 1993.